The Astronomical Journal, 134:1133–1144, 2007 September


# FRACTION OF CONTACT BINARY TROJAN ASTEROIDS

Rita K. Mann, David Jewitt, and Pedro Lacerda
Institute for Astronomy, University of Hawaii, 2680 Woodlawn Drive, Honolulu, HI 96822, USA;
rmann@ifa.hawaii.edu, jewitt@ifa.hawaii.edu, pedro@ifa.hawaii.edu
*Received 2006 October 6; accepted 2007 May 22*

## ABSTRACT

We present the results of an optical light-curve survey of 114 Jovian Trojan asteroids conducted to determine the fraction of contact binaries. Sparse sampling was used to assess the photometric range of the asteroids, and those showing the largest ranges were targeted for detailed follow-up observations. This survey led to the discovery of two Trojan asteroids, (17365) and (29314), displaying large light-curve ranges ($\sim$1 mag) and long rotation periods ($<$2 rotations day$^{-1}$) consistent with a contact binary nature. The optical light curves of both asteroids are well matched by Roche binary equilibrium models. Using these binary models, we find low densities of $\sim$600 and 800 kg m$^{-3}$, suggestive of porous interiors. The fraction of contact binaries is estimated to be between 6% and 10%, comparable to the fraction in the Kuiper Belt. The total binary fraction in the Trojan clouds (including both wide and close pairs) must be higher.

*Key words:* minor planets, asteroids — solar system: general — surveys

*Online material:* machine-readable tables

## 1. INTRODUCTION

The existence and importance of binary asteroids in small-body populations has only been realized in the last decade, after the first unambiguous detection of a satellite around main-belt asteroid 243 Ida by the *Galileo* spacecraft (Belton et al. 1995; Chapman et al. 1995). It is now evident that binaries exist in the main-belt asteroids, the near-Earth asteroids, and the Kuiper Belt (see review by Richardson & Walsh 2006 and references therein). Apart from spacecraft flybys (and the rare case of measuring gravitational perturbations of planets by very large asteroids), studying the orbital dynamics of binary systems provides the only method available for calculating mass and density. Density measurements are important as probes of internal structure, enabling constraints to be placed on the porosity and composition.

The Jovian Trojan asteroids are trapped in a 1:1 mean motion resonance with Jupiter. They form two large clouds around the stable (L4, L5) Lagrangian points 60° ahead of and behind the giant planet. It has been estimated that $\sim 10^5$ Trojan asteroids with diameters larger than 1 km exist (Jewitt et al. 2000; Yoshida & Nakamura 2005), comparable in number to the main-belt population ($6.7 \times 10^5$ asteroids; Ivezic et al. 2001), making it clear that they comprise an important reservoir of information. The Trojan asteroids of Jupiter have yet to be searched systematically for the presence of binaries. Despite this fact, two Trojan binaries have already been identified: 617 Patroclus, a resolved wide binary discovered by Merline et al. (2001), and 624 Hektor, which has a distinctive light curve that indicates it is a close or contact binary (Cook 1971; Hartmann et al. 1988) and a widely separated satellite, has recently been imaged (Marchis et al. 2006a). The Trojans are intriguing because they show larger photometric ranges when compared with main-belt asteroids (Hartmann et al. 1988), particularly those with diameters larger than 90 km (Binzel & Sauter 1992). Large light-curve amplitudes suggest elongated shapes or binarity.

While it is not clear whether the Trojans formed at their current location alongside Jupiter or were trapped after forming at larger heliocentric distances (Morbidelli et al. 2005), it is believed that these bodies are primordial. Understanding their composition and internal structure is therefore of great interest, making density determination vital. The density of Trojan 617 Patroclus has been estimated as $\rho = 800^{+200}_{-100}$ kg m$^{-3}$ based on the measured orbital period and size and on diameter determinations made from infrared data (Marchis et al. 2006b). This low density contrasts with a comparatively high estimate for 624 Hektor, namely, $\rho = 2480^{+290}_{-80}$ kg m$^{-3}$, determined from the light curve and a Roche binary model (Lacerda & Jewitt 2007).

Close or contact binaries are composed of two asteroids in a tight orbit around each other. The Trojan contact binary fraction is potentially important in distinguishing between various formation theories. For example, one model of binary formation by dynamical friction predicts that close binaries should be common (Goldreich et al. 2002), while another based on three-body interactions asserts that they should be rare (Weidenschilling 2002). The nature of the Trojan binaries can also reveal clues about their formation. It is known that different mechanisms formed binaries in the main belt and the Kuiper Belt because of the distinct types of binaries found in both populations. It is suspected that gravitational processes predominantly form Kuiper Belt binaries, the known examples of which have components of comparable mass and large separations (Weidenschilling 2002; Goldreich et al. 2002; Funato et al. 2004; Astakhov et al. 2005). Subcatastrophic impacts followed by gravitational interaction with the debris formed are the leading way to form tight binary systems with unequal mass components that make up the larger main-belt binary population (Weidenschilling 1989; Richardson & Walsh 2006). A comparative study of the binaries in the Trojan clouds, the main belt, and the Kuiper Belt might illuminate the different roles played by formation conditions in these populations.

Motivated by the lack of studies about Trojan binaries, the aim of this paper is to investigate the fraction of close or contact binary systems among the Jovian Trojan population. Contact binaries are specifically targeted for the ease with which they can be identified using optical light-curve information. Here we present a technique called "sparse sampling," which we used to conduct a light-curve survey of 114 Jovian Trojan asteroids. The results of this survey, the discovery of two suspected contact binary asteroids, and a

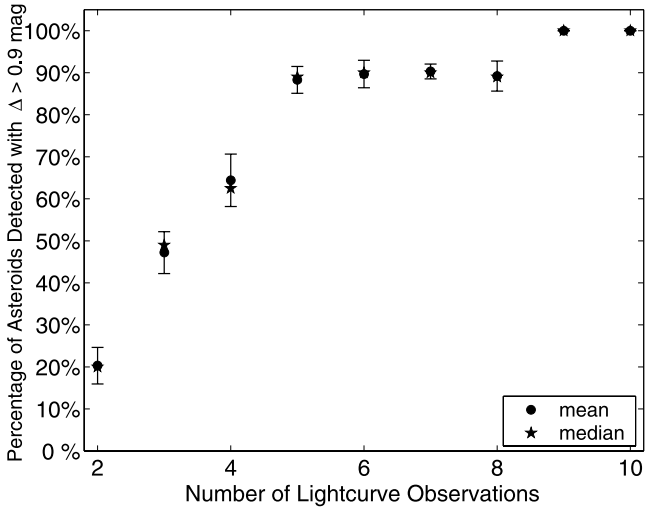


FIG. 1.—Percentage of asteroids detected with photometric ranges greater than 0.9 mag vs. number of light-curve observations. Monte Carlo simulations were conducted on a sample of asteroids with a photometric range of 1.2 mag and single-peaked light-curve periods between 3 and 10 hr to determine sparse-sampling efficiency.

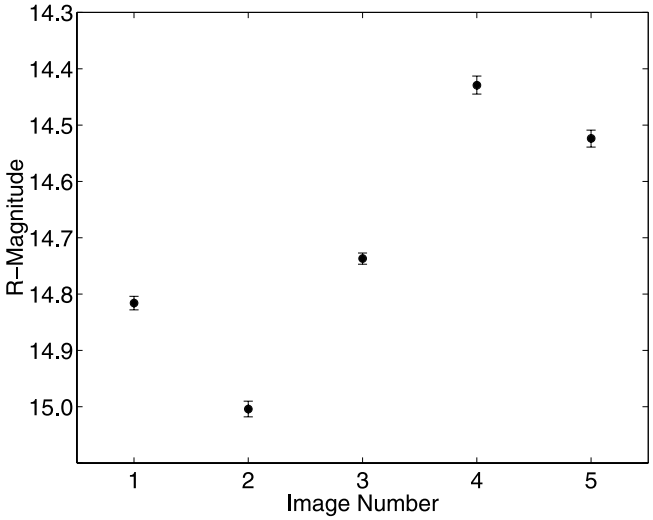


FIG. 2.—Sparse-sampled *R*-band photometry of 944 Hidalgo. The photometric range estimated from five observations is 0.58 ± 0.02 mag, consistent with previous measurements of 0.60 mag from Harris et al. (2006).

discussion of the binary fraction in the Jovian Trojan population follow.

## 2. OBSERVATIONS

### 2.1. *Sparse Sampling*

The maximum photometric range that can be exhibited by a rotationally elongated, strengthless body is 0.9 mag (Leone et al. 1984). Ranges larger than 0.9 mag are strongly suggestive of a contact binary nature, in which mutual gravitational deformation of the components can drive the range up to ~1.2 mag (Weidenschilling 1980; Leone et al. 1984). In principle, structurally strong bodies can maintain any shape and show an arbitrarily large photometric range. However, most main-belt asteroids larger than ~150 m in diameter show little sign of possessing internal strength sufficient to resist gravity and/or rotational deformation (Pravec et al. 2002; Holsapple 2004), and we expect that the Trojan asteroids are similarly structurally weak. In what follows, we assume that objects with a photometric range >0.9 mag are candidate contact binaries.

To examine the efficiency of sparse light-curve sampling, we conducted a series of Monte Carlo tests. The tests were applied to asteroids with a photometric range of 1.2 mag and double-peaked light-curve periods uniformly distributed between 6 and 20 hr. The light curves were uniformly sampled by $N = 1, 2 \ldots 10$ observations over one night. Asteroids for which the sparse-sampling technique detected photometric ranges between 0.9 and 1.2 mag were picked out as successful candidates. Monte Carlo simulations suggest that between 85% and 92% of asteroids with photometric ranges of 1.2 mag would be identified as contact binary candidates from just five measurements of brightness per night (see Fig. 1). (The efficiency of detecting brightness variations larger than 0.9 mag ranged from ~71% for asteroids with actual peak-to-peak light-curve amplitudes of 1.0 mag to ~81% for asteroids with peak-to-peak amplitudes of 1.1 mag.) The simulations indicate that the accuracy with which contact binary candidates are identified varies little when sampling between five and eight light-curve points per asteroid (see Fig. 1). The advantage of sparse sampling is clear: estimates of photometric range for a large number of asteroids can be made rapidly, significantly reducing observing time. Asteroids exhibiting large photometric ranges in the sparse-sampling study are subsequently targeted for detailed follow-up observations with dense coverage in rotational phase space.

To further test the sparse-sampling technique, we observed 2674 Pandarus and 944 Hidalgo, two asteroids known to show large photometric variations. From published light curves, 2674 Pandarus is known to have a photometric range of 0.49 mag (Hartmann et al. 1988). Using the sparse-sampling technique, with the same sampling as for all other asteroids in the study (and without prior knowledge of the rotational phase), we measured a light-curve amplitude of 0.50 ± 0.01 mag for Pandarus. Hidalgo has shown a maximum photometric variation of 0.60 mag (Harris et al. 2006), whereas sparse sampling measured the brightness range to be 0.58 ± 0.02 mag (see Figs. 2 and 3). The agreement results show that the photometric range can be usefully estimated with only five measurements of asteroid brightness.

Having gained confidence in the technique through simulations and observational tests, we applied sparse sampling to the

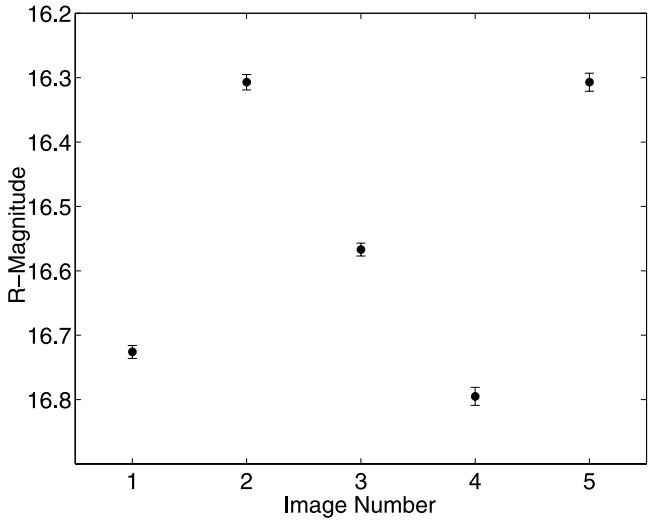


FIG. 3.—Sparse-sampled *R*-band photometry of 2674 Pandarus. The photometric range estimated from five observations is 0.50 ± 0.01 mag, consistent with previous measurements of 0.49 mag (Hartmann et al. 1988).

TABLE 1
JOURNAL OF OBSERVATIONS

| UT Date | Telescope | Seeing (arcsec) | Project[a] | Full/Half Night | Comments |
|---|---|---|---|---|---|
| 2005 Mar 7 | LOT 1 m | 2.0 | Sparse | Full | Scattered cirrus |
| 2005 Mar 9 | LOT 1 m | 2.2 | Sparse | Full | Windy |
| 2005 Mar 11 | LOT 1 m | 2.0 | Sparse | Half | Cloudy |
| 2005 Mar 13 | LOT 1 m | 1.7 | Sparse | Full | Clear skies |
| 2005 Apr 5 | UH 2.2 m | 0.6 | Sparse | Full | Cirrus |
| 2005 Apr 6 | UH 2.2 m | 0.6–0.8 | Sparse | Half | Cloudy |
| 2005 Apr 7 | UH 2.2 m | 0.6 | Sparse | Half | Photometric |
| 2005 Apr 9 | UH 2.2 m | 0.6–0.7 | Sparse | Half | Clear |
| 2005 Apr 11 | UH 2.2 m | 0.6 | Sparse | Half | Clear |
| 2005 Apr 12 | UH 2.2 m | 0.7 | Sparse | Half | Clear |
| 2005 Apr 14 | UH 2.2 m | 0.7 | Sparse | Half | Clear |
| 2005 Apr 15 | UH 2.2 m | 0.8 | Sparse | Half | Cloudy |
| 2005 Apr 17 | UH 2.2 m | 0.8 | Dense | Half | Cloudy |
| 2005 Apr 18 | UH 2.2 m | 0.8–1.0 | Dense | Half | Moon rising |
| 2006 Feb 1 | UH 2.2 m | 1.0 | Dense | Full | Focus problems |
| 2006 Feb 2 | UH 2.2 m | 0.6 | Dense | Full | Clear |
| 2006 Feb 4 | UH 2.2 m | 1.5 | Dense | Full | Strong winds |
| 2006 Feb 24 | UH 2.2 m | 1.0–1.2 | Dense | Full | Windy |
| 2006 Apr 24 | UH 2.2 m | 0.7 | Dense | Half | Cloudy/clear |
| 2006 Apr 29 | UH 2.2 m | 0.8 | Dense | Half | Clear, windy |
| 2006 Apr 30 | UH 2.2 m | 0.9 | Dense | Half | Clear, windy |
| 2006 May 1 | UH 2.2 m | 0.9–1.0 | Dense | Half | Windy |

[a] Sparse sampling survey or follow-up densely sampled light curves.

Trojan asteroids. Taking five short exposures, while cycling through the asteroids, we were able to obtain limited sampling of 114 asteroid light curves in nine good-weather nights of observing.

### 2.2. *Data Acquisition and Reduction*

We obtained sparsely sampled optical light-curve data for the Jovian Trojan asteroids using both the University of Hawaii (UH) 2.2 m telescope on Mauna Kea and the Lulin 1 m Telescope (LOT) in Taiwan. We used a $2048 \times 2048$ pixel Tektronix charge-coupled device (CCD) on the 2.2 m telescope. This detector has a $0.219''$ pixel$^{-1}$ image scale and a field of view of 7.5 arcmin$^2$. The CCD on LOT (VersArray: 1300B) has $1340 \times 1300$ pixels with a $0.516''$ pixel$^{-1}$ scale and a field of view of $11.5' \times 11.2'$. All images were taken in the *R* band with exposure times scaled to the brightnesses of the asteroids. On LOT, the exposure times ranged from 30 s for objects brighter than 15 mag up to 120 s for 19 mag Trojans. At the 2.2 m telescope, the exposure times ranged from 10 s for objects brighter than 17 mag to 150 s for 20 mag asteroids. See Table 1 for a description of the observations.

Raw data frames were bias-subtracted, then flat-fielded using a master flat field produced from median-filtering dithered images of the sky taken at dusk and dawn. Landolt (1992) standard star fields were imaged and measured to convert the instrumental magnitudes to an absolute magnitude scale. An aperture radius of 8 pixels was consistently used throughout the observations for images taken on both telescopes. Median sky values were determined using an adjacent annulus around the aperture with an outer radius of 20 pixels. The reason for the similar aperture and sky annulus sizes on both telescopes, despite differing pixel scales, was the significantly worse seeing conditions at Lulin (see Table 1). For the sparse-sampling survey, two images were taken in each setting and then averaged to obtain the brightness measurement. The photometric uncertainties were small ($\leq$0.02 mag) compared to the photometric variability that is the subject of interest, and so we have ignored these uncertainties in our presentation of the data. For the densely sampled light curves, errors for each observation were calculated using Poisson statistics. The instrumental magnitude of the asteroid in each image was subtracted from the brightness of a nearby field star. The field star was chosen to be persistent in all five observations and helped reduce photometric errors by providing a correction for weather variations occurring throughout the night. Images in which the asteroid was affected by proximity to a field star were rejected and resulted in some Trojans having only four measurements of brightness, rather than five.

## 3. RESULTS

Tables 2 and 3 contain results of the sparsely sampled light-curve survey. In Table 2 the average *R*-band magnitude, $\overline{m}_R$, is listed, along with the independent measurements of the asteroid's brightness, expressed as deviations from the mean magnitude. The last column shows the maximum deviation measured, which gives a lower limit to the photometric range of each asteroid. Table 3 contains the absolute magnitude, $m_R(1, 1, 0)$, which is defined as the magnitude an object would have if placed at heliocentric ($r$) and geocentric ($\Delta$) distances of 1 AU and at a phase angle of $\alpha = 0^\circ$. The conversion between the apparent magnitude, $m_R$, and absolute magnitude, $m_R(1, 1, 0)$, is

$$m_R(1, 1, 0) = m_R - 5 \log (r\Delta) - \beta\alpha, \quad (1)$$

where $\beta$ is the phase coefficient for which we used a value of 0.04 mag deg$^{-1}$ for the low-albedo Trojan asteroids (Bowell et al. 1989). Also listed in Table 3 is an estimate of the equivalent circular diameter, $D_e$, which was calculated using (Russell 1916)

$$m_R(1, 1, 0) = m_\odot - 2.5 \log\left(\frac{pD_e^2}{4 \times 2.25 \times 10^{16}}\right). \quad (2)$$

Here $p$ is the geometric albedo, for which a value of 0.04 was used throughout (Fernandez et al. 2003), and $m_\odot = -27.1$ is the apparent red magnitude of the Sun (Cox 2000, p. 341).

TABLE 2

PHOTOMETRY OF JOVIAN TROJAN ASTEROIDS

| Trojans | Telescope | $\bar{m}_R$[a] | $m_1 - \bar{m}_R$[b] | $m_2 - \bar{m}_R$[b] | $m_3 - \bar{m}_R$[b] | $m_4 - \bar{m}_R$[b] | $m_5 - \bar{m}_R$[b] | $\Delta m_R$[c] |
|---|---|---|---|---|---|---|---|---|
| 884 | UH | 16.37 | 0.13 | −0.09 | −0.07 | 0.08 | −0.05 | 0.22 |
| 1172 | UH | 15.78 | 0.06 | −0.05 | −0.04 | 0.03 | ... | 0.11 |
| 1173 | LOT | 16.85 | 0.02 | −0.20 | −0.08 | 0.17 | 0.10 | 0.37 |
| 1208 | UH | 16.60 | 0.06 | 0.06 | −0.01 | 0.00 | −0.06 | 0.12 |
| 1583 | UH | 16.87 | −0.02 | −0.07 | 0.00 | 0.04 | 0.04 | 0.11 |
| 1647 | UH | 18.88 | −0.20 | −0.14 | 0.09 | 0.24 | ... | 0.44 |
| 1867 | UH | 15.82 | 0.04 | 0.04 | 0.02 | −0.07 | −0.04 | 0.12 |
| 1868 | UH | 17.52 | 0.03 | −0.03 | −0.08 | 0.06 | 0.02 | 0.14 |
| 1869 | UH | 19.51 | −0.18 | 0.01 | 0.03 | 0.07 | 0.08 | 0.26 |
| 1870 | UH | 17.90 | −0.05 | −0.01 | 0.05 | −0.03 | 0.03 | 0.10 |
| 1871 | UH | 19.29 | 0.05 | 0.05 | 0.01 | −0.07 | −0.04 | 0.12 |
| 1872 | LOT | 17.99 | 0.09 | −0.03 | −0.01 | 0.01 | −0.06 | 0.15 |
| 1873 | UH | 17.24 | −0.14 | −0.05 | 0.11 | 0.08 | ... | 0.25 |
| 2146 | UH | 17.79 | −0.07 | 0.07 | 0.05 | −0.06 | 0.00 | 0.14 |
| 2207 | UH | 16.03 | 0.05 | −0.02 | −0.03 | 0.03 | −0.03 | 0.08 |
| 2241 | UH | 15.95 | 0.11 | −0.15 | 0.01 | 0.03 | ... | 0.26 |
| 2260 | UH | 17.47 | 0.03 | 0.12 | −0.09 | −0.03 | −0.03 | 0.22 |
| 2357 | UH | 15.93 | 0.01 | 0.04 | −0.02 | −0.03 | ... | 0.07 |
| 2357 | LOT | 15.96 | −0.02 | −0.01 | −0.01 | 0.02 | 0.03 | 0.05 |
| 2363 | UH | 17.12 | 0.03 | 0.03 | −0.06 | 0.01 | ... | 0.09 |
| 2674 | LOT | 16.54 | 0.19 | −0.23 | 0.03 | 0.26 | −0.23 | 0.49 |
| 2893 | UH | 16.62 | 0.14 | −0.03 | −0.11 | 0.00 | ... | 0.26 |
| 2895 | UH | 17.24 | −0.01 | −0.04 | 0.08 | −0.02 | ... | 0.12 |
| 2895 | LOT | 16.73 | −0.02 | 0.05 | 0.01 | −0.01 | −0.04 | 0.09 |
| 2920 | UH | 16.57 | 0.10 | 0.06 | −0.10 | −0.06 | ... | 0.20 |
| 3240 | UH | 18.06 | −0.09 | −0.17 | 0.01 | −0.15 | 0.40 | 0.57 |
| 3317 | UH | 16.33 | 0.02 | 0.01 | −0.05 | −0.01 | 0.04 | 0.09 |
| 3451 | UH | 15.91 | −0.10 | 0.14 | 0.04 | −0.02 | −0.06 | 0.25 |
| 3708 | UH | 17.20 | 0.01 | −0.04 | −0.01 | 0.01 | 0.02 | 0.06 |
| 3709 | UH | 17.42 | −0.05 | −0.04 | 0.01 | −0.05 | 0.13 | 0.18 |
| 4068 | UH | 17.41 | −0.07 | −0.06 | 0.04 | 0.04 | 0.04 | 0.11 |
| 4348 | UH | 17.09 | 0.13 | 0.10 | −0.03 | −0.01 | −0.01 | 0.16 |
| 4489 | LOT | 17.04 | 0.08 | −0.01 | −0.06 | −0.01 | ... | 0.13 |
| 4707 | LOT | 17.81 | −0.18 | 0.16 | −0.10 | −0.08 | 0.21 | 0.40 |
| 4708 | LOT | 17.35 | −0.20 | 0.13 | −0.04 | 0.11 | ... | 0.33 |
| 4709 | UH | 15.92 | −0.05 | 0.05 | 0.09 | −0.05 | −0.06 | 0.15 |
| 4715 | LOT | 17.13 | 0.17 | −0.23 | −0.13 | 0.23 | −0.03 | 0.46 |
| 4722 | LOT | 17.28 | −0.02 | 0.00 | 0.01 | −0.04 | 0.05 | 0.08 |
| 4754 | LOT | 16.95 | 0.02 | 0.00 | 0.01 | −0.01 | −0.01 | 0.03 |
| 4792 | UH | 17.85 | 0.01 | 0.01 | 0.01 | −0.03 | ... | 0.05 |
| 4792 | LOT | 17.56 | 0.17 | 0.03 | −0.10 | −0.06 | −0.04 | 0.27 |
| 4805 | UH | 17.73 | 0.01 | 0.04 | 0.04 | −0.09 | ... | 0.14 |
| 4827 | UH | 17.86 | 0.01 | 0.07 | 0.02 | −0.06 | −0.05 | 0.13 |
| 4828 | UH | 17.63 | 0.13 | 0.11 | −0.06 | −0.19 | ... | 0.32 |
| 4828 | LOT | 17.47 | 0.06 | 0.00 | −0.11 | 0.06 | ... | 0.18 |
| 4832 | LOT | 17.55 | 0.01 | 0.00 | 0.01 | 0.00 | −0.02 | 0.03 |
| 4833 | UH | 17.25 | −0.18 | 0.10 | 0.13 | 0.05 | −0.10 | 0.31 |
| 4834 | UH | 17.70 | 0.06 | 0.02 | −0.02 | −0.04 | −0.03 | 0.10 |
| 4867 | LOT | 16.97 | 0.02 | −0.01 | −0.02 | −0.03 | 0.04 | 0.07 |
| 5119 | UH | 17.97 | 0.07 | 0.07 | −0.02 | −0.11 | ... | 0.18 |
| 5233 | UH | 18.85 | 0.00 | −0.08 | 0.06 | 0.02 | ... | 0.15 |
| 5648 | UH | 17.84 | 0.06 | 0.02 | −0.03 | −0.05 | ... | 0.11 |
| 6002 | UH | 18.00 | 0.06 | 0.03 | −0.02 | −0.07 | ... | 0.13 |
| 9030 | UH | 18.20 | −0.21 | 0.06 | 0.36 | −0.08 | −0.13 | 0.57 |
| 9142 | LOT | 18.19 | −0.08 | 0.05 | 0.04 | −0.01 | −0.01 | 0.13 |
| 9431 | LOT | 18.19 | 0.07 | −0.01 | −0.12 | −0.06 | 0.13 | 0.25 |
| 9694 | UH | 17.90 | −0.05 | −0.16 | −0.02 | 0.08 | 0.15 | 0.32 |
| 11554 | LOT | 17.31 | 0.03 | 0.00 | −0.03 | 0.00 | −0.01 | 0.06 |
| 11668 | UH | 19.33 | −0.05 | −0.02 | 0.14 | −0.03 | −0.08 | 0.22 |
| 12649 | UH | 19.64 | 0.04 | 0.00 | −0.06 | 0.00 | 0.02 | 0.10 |
| 13402 | UH | 19.08 | −0.02 | 0.00 | 0.00 | 0.02 | 0.01 | 0.04 |
| 15527 | LOT | 18.50 | 0.05 | 0.29 | −0.13 | −0.20 | ... | 0.49 |
| 16667 | UH | 19.02 | −0.11 | 0.06 | 0.05 | 0.01 | 0.00 | 0.17 |
| 17172 | LOT | 17.83 | 0.04 | 0.03 | −0.04 | 0.00 | −0.03 | 0.07 |
| 17365 | LOT | 17.61 | −0.21 | 0.35 | 0.05 | −0.20 | ... | 0.56 |

TABLE 2—*Continued*

| Trojans | Telescope | $\bar{m}_R$[a] | $m_1 - \bar{m}_R$[b] | $m_2 - \bar{m}_R$[b] | $m_3 - \bar{m}_R$[b] | $m_4 - \bar{m}_R$[b] | $m_5 - \bar{m}_R$[b] | $\Delta m_R$[c] |
|---|---|---|---|---|---|---|---|---|
| 17419 | UH | 18.76 | −0.03 | 0.00 | 0.00 | 0.02 | 0.02 | 0.05 |
| 17442 | UH | 19.39 | 0.11 | 0.00 | 0.06 | −0.04 | −0.13 | 0.24 |
| 17492 | UH | 17.70 | 0.09 | 0.10 | 0.03 | −0.05 | −0.16 | 0.26 |
| 18037 | UH | 19.22 | −0.05 | −0.06 | −0.03 | −0.01 | 0.15 | 0.21 |
| 18054 | UH | 18.22 | −0.06 | 0.02 | −0.01 | −0.01 | 0.05 | 0.11 |
| 23463 | UH | 19.15 | −0.07 | 0.01 | 0.08 | −0.04 | 0.02 | 0.15 |
| 23549 | UH | 18.90 | −0.03 | 0.02 | 0.09 | 0.00 | −0.08 | 0.16 |
| 24018 | UH | 19.19 | 0.09 | 0.02 | −0.18 | −0.11 | 0.17 | 0.35 |
| 24022 | UH | 19.79 | 0.06 | −0.08 | −0.06 | 0.08 | ... | 0.16 |
| 24449 | UH | 19.50 | 0.13 | 0.08 | −0.17 | −0.17 | 0.13 | 0.30 |
| 24451 | UH | 18.19 | 0.04 | 0.00 | 0.05 | −0.01 | −0.07 | 0.12 |
| 24452 | UH | 19.06 | −0.03 | 0.03 | −0.03 | 0.01 | 0.01 | 0.06 |
| 24456 | UH | 19.37 | −0.15 | 0.10 | 0.13 | 0.04 | −0.11 | 0.27 |
| 24531 | LOT | 19.72 | 0.25 | −0.07 | 0.05 | 0.00 | −0.23 | 0.48 |
| 25344 | UH | 19.22 | 0.13 | 0.01 | −0.13 | −0.11 | 0.09 | 0.26 |
| 25347 | UH | 19.23 | 0.09 | 0.20 | 0.04 | −0.16 | −0.17 | 0.37 |
| 29314 | UH | 19.44 | 0.22 | 0.31 | 0.21 | −0.21 | −0.53 | 0.83 |
| 30498 | UH | 19.59 | 0.00 | −0.07 | −0.12 | 0.10 | 0.09 | 0.22 |
| 30499 | UH | 19.76 | 0.05 | −0.03 | 0.04 | −0.07 | 0.01 | 0.12 |
| 30505 | UH | 19.02 | −0.13 | 0.15 | 0.08 | −0.22 | 0.12 | 0.34 |
| 30506 | UH | 18.78 | −0.19 | −0.18 | −0.02 | 0.19 | 0.20 | 0.39 |
| 30704 | UH | 18.67 | −0.08 | −0.03 | −0.01 | 0.11 | ... | 0.19 |
| 30942 | UH | 18.52 | 0.04 | 0.02 | 0.00 | −0.02 | −0.04 | 0.08 |
| 31806 | UH | 19.51 | 0.15 | 0.07 | −0.09 | −0.03 | −0.10 | 0.25 |
| 31814 | UH | 19.81 | −0.11 | 0.11 | 0.23 | −0.09 | −0.16 | 0.39 |
| 31819 | UH | 18.90 | 0.20 | 0.01 | 0.00 | −0.03 | −0.17 | 0.37 |
| 31820 | UH | 20.06 | 0.16 | 0.09 | 0.05 | 0.12 | −0.40 | 0.56 |
| 32482 | LOT | 18.68 | 0.13 | −0.14 | 0.13 | 0.03 | −0.15 | 0.27 |
| 32496 | UH | 18.01 | 0.01 | −0.01 | −0.01 | 0.02 | −0.02 | 0.04 |
| 32811 | UH | 18.43 | −0.11 | −0.02 | 0.01 | 0.05 | 0.07 | 0.18 |
| 47962 | UH | 19.59 | 0.04 | −0.05 | −0.02 | 0.00 | 0.03 | 0.09 |
| 51364 | UH | 18.49 | 0.02 | 0.05 | 0.04 | −0.01 | −0.09 | 0.15 |
| 53436 | UH | 18.40 | −0.03 | 0.02 | 0.00 | 0.00 | 0.01 | 0.04 |
| 55060 | LOT | 18.85 | 0.27 | −0.09 | −0.22 | 0.03 | ... | 0.48 |
| 55419 | LOT | 18.68 | 0.01 | −0.22 | −0.05 | 0.20 | 0.06 | 0.42 |
| 65216 | UH | 19.67 | 0.14 | −0.02 | −0.05 | −0.03 | −0.03 | 0.19 |
| 67065 | UH | 18.99 | 0.08 | −0.12 | −0.09 | 0.09 | 0.04 | 0.21 |
| 69437 | UH | 19.54 | −0.06 | 0.01 | 0.01 | 0.02 | 0.01 | 0.08 |
| 73677 | UH | 19.34 | 0.06 | 0.03 | 0.00 | −0.02 | −0.01 | 0.08 |
| 85798 | UH | 19.10 | −0.08 | 0.03 | 0.02 | 0.03 | 0.00 | 0.12 |
| 1999 XJ55 | UH | 19.29 | 0.04 | 0.00 | −0.03 | −0.01 | ... | 0.06 |
| 2000 TG61 | UH | 19.76 | 0.01 | −0.01 | 0.00 | 0.02 | −0.03 | 0.04 |
| 2000 SJ350 | UH | 20.17 | −0.20 | −0.14 | −0.13 | 0.15 | 0.08 | 0.35 |
| 2001 QZ113 | UH | 19.53 | −0.02 | −0.02 | −0.02 | 0.00 | 0.05 | 0.07 |
| 2001 XW71 | UH | 20.24 | 0.06 | −0.03 | −0.05 | 0.17 | −0.08 | 0.24 |
| 2001 QQ199 | UH | 20.51 | −0.12 | −0.09 | 0.04 | 0.05 | 0.11 | 0.23 |
| 2004 BV84 | UH | 20.34 | 0.05 | −0.01 | 0.01 | −0.05 | ... | 0.10 |
| 2004 FX147 | UH | 19.67 | 0.06 | −0.16 | −0.13 | 0.02 | 0.20 | 0.36 |
| 2005 EJ133 | UH | 20.15 | −0.11 | 0.01 | 0.00 | 0.08 | 0.01 | 0.18 |

NOTE.—Table 2 is also available in machine-readable form in the electronic edition of the *Astronomical Journal*.

[a] Mean *R*-band magnitude.

[b] *R*-band magnitude minus mean *R*-band magnitude.

[c] Photometric range.

Figure 4 shows the distribution of photometric ranges shown by the Trojan asteroids in the sparsely sampled light-curve survey. For comparison, Figure 5 shows the photometric range distributions of both the Trojan and main-belt asteroids with diameters between 70 and 150 km (main-belt asteroid data taken from Barucci et al. 2002). Figure 5 reveals that a larger fraction of Trojan asteroids have photometric ranges larger than main-belt asteroids, similar to previous studies by Hartmann et al. (1988). A Kolmogorov-Smirnov statistical test found a 32.1% probability that the two distributions are drawn from the same parent distribution.

Trojan asteroids (17365) and (29314) showed the largest photometric ranges in the sparsely sampled photometry, with $0.56 \pm 0.02$ and $0.83 \pm 0.03$ mag, respectively (see Table 2). Follow-up observations to obtain densely sampled optical light curves for both Trojan asteroids were taken using the UH 2.2 m telescope between 2005 April 9 and 17. We were unable to complete the observations due to bad weather coupled with the fact that the asteroids were quickly setting. We were, however, able to confirm the large photometric ranges to motivate further study of these Trojan asteroids (see Figs. 6–9). In our first dense light-curve study, in 2005, asteroid (17365) had a photometric range of

TABLE 3

Geometric and Photometric Properties of Jovian Trojan Asteroids

| Trojan | $m_R(1,1,0)$[a] | $r$[b] (AU) | $\Delta$[c] (AU) | $\alpha$[d] (deg) | $D_e$[e] (km) | L4/L5 |
|---|---|---|---|---|---|---|
| 884 | 8.53 | 5.66 | 5.34 | 9.9 | 146 | L5 |
| 1172 | 8.00 | 5.68 | 5.24 | 9.4 | 193 | L5 |
| 1173 | 9.08 | 6.02 | 5.27 | 6.6 | 150 | L5 |
| 1208 | 8.86 | 5.69 | 5.17 | 9.0 | 134 | L5 |
| 1583 | 9.30 | 5.33 | 4.92 | 10.2 | 99 | L4 |
| 1647 | 11.50 | 5.20 | 4.70 | 10.1 | 37 | L4 |
| 1867 | 8.18 | 5.34 | 5.12 | 10.7 | 163 | L5 |
| 1868 | 9.91 | 5.50 | 5.00 | 9.5 | 80 | L4 |
| 1869 | 12.10 | 5.49 | 4.75 | 7.5 | 34 | L4 |
| 1870 | 10.29 | 5.42 | 5.03 | 10.1 | 64 | L5 |
| 1871 | 11.47 | 5.46 | 5.46 | 10.5 | 36 | L5 |
| 1872 | 10.78 | 5.51 | 4.61 | 4.7 | 84 | L5 |
| 1873 | 9.71 | 5.11 | 5.02 | 11.3 | 78 | L5 |
| 2146 | 9.98 | 5.69 | 5.28 | 9.6 | 77 | L4 |
| 2207 | 8.73 | 5.05 | 4.61 | 10.7 | 127 | L5 |
| 2241 | 8.34 | 5.17 | 5.17 | 11.1 | 148 | L5 |
| 2260 | 9.92 | 5.39 | 4.92 | 9.8 | 77 | L4 |
| 2357 | 8.34 | 5.29 | 4.90 | 10.4 | 149 | L5 |
| 2357 | 8.79 | 5.29 | 4.51 | 7.1 | 164 | L5 |
| 2363 | 9.74 | 5.24 | 4.69 | 9.7 | 85 | L5 |
| 2674 | 9.37 | 5.17 | 4.49 | 8.6 | 111 | L5 |
| 2893 | 8.75 | 5.56 | 5.50 | 10.4 | 128 | L5 |
| 2895 | 9.79 | 5.25 | 4.69 | 9.6 | 81 | L5 |
| 2895 | 9.67 | 5.24 | 4.39 | 6.3 | 118 | L5 |
| 2920 | 9.23 | 5.25 | 4.64 | 9.3 | 111 | L4 |
| 3240 | 10.04 | 5.92 | 5.61 | 9.5 | 75 | L5 |
| 3317 | 8.44 | 5.78 | 5.39 | 9.5 | 157 | L5 |
| 3451 | 8.38 | 5.44 | 4.90 | 9.4 | 163 | L5 |
| 3708 | 9.29 | 5.93 | 5.41 | 8.6 | 113 | L5 |
| 3709 | 9.77 | 5.58 | 5.04 | 9.1 | 87 | L4 |
| 4068 | 9.97 | 5.33 | 4.78 | 9.5 | 78 | L4 |
| 4348 | 9.51 | 5.49 | 4.95 | 9.2 | 97 | L5 |
| 4489 | 9.26 | 5.54 | 5.37 | 10.3 | 104 | L4 |
| 4707 | 10.60 | 5.53 | 4.62 | 4.4 | 96 | L5 |
| 4708 | 10.05 | 5.34 | 4.65 | 8.2 | 84 | L5 |
| 4709 | 8.53 | 5.30 | 4.71 | 9.3 | 153 | L5 |
| 4715 | 9.85 | 5.30 | 4.62 | 8.4 | 91 | L5 |
| 4722 | 10.04 | 5.44 | 4.60 | 6.0 | 102 | L5 |
| 4754 | 10.04 | 5.22 | 4.29 | 4.1 | 129 | L5 |
| 4792 | 10.00 | 5.69 | 5.25 | 9.5 | 74 | L5 |
| 4792 | 10.11 | 5.68 | 4.86 | 6.1 | 98 | L5 |
| 4805 | 10.06 | 5.46 | 5.11 | 10.2 | 71 | L5 |
| 4827 | 10.51 | 5.08 | 4.70 | 10.9 | 55 | L5 |
| 4828 | 10.18 | 4.96 | 4.81 | 11.6 | 59 | L5 |
| 4828 | 10.37 | 4.96 | 4.40 | 10.1 | 63 | L5 |
| 4832 | 10.00 | 5.94 | 5.03 | 4.2 | 128 | L5 |
| 4833 | 9.58 | 5.61 | 5.07 | 9.1 | 95 | L4 |
| 4834 | 9.80 | 5.94 | 5.38 | 8.4 | 91 | L4 |
| 4867 | 9.86 | 5.20 | 4.43 | 7.4 | 97 | L5 |
| 5119 | 10.08 | 5.74 | 5.30 | 9.3 | 72 | L5 |
| 5233 | 11.32 | 5.05 | 4.92 | 11.4 | 35 | L5 |
| 5648 | 9.76 | 5.88 | 5.62 | 9.7 | 82 | L5 |
| 6002 | 10.34 | 5.55 | 4.97 | 8.9 | 66 | L5 |
| 9030 | 11.03 | 5.11 | 4.46 | 9.1 | 49 | L5 |
| 9142 | 10.41 | 5.84 | 5.27 | 8.4 | 70 | L5 |
| 9431 | 10.51 | 5.52 | 5.17 | 10.0 | 59 | L4 |
| 9694 | 10.75 | 5.39 | 4.51 | 5.5 | 78 | L4 |
| 11554 | 10.12 | 5.32 | 4.53 | 6.9 | 90 | L5 |
| 11668 | 11.74 | 5.87 | 5.04 | 5.9 | 47 | L4 |
| 12649 | 11.61 | 5.90 | 5.58 | 9.5 | 36 | L5 |
| 13402 | 11.20 | 5.72 | 5.35 | 9.6 | 43 | L5 |
| 15527 | 10.95 | 5.32 | 5.01 | 10.5 | 47 | L4 |
| 16667 | 10.85 | 6.17 | 5.88 | 9.1 | 54 | L5 |
| 17172 | 10.59 | 5.45 | 4.61 | 6.0 | 80 | L5 |
| 17365 | 10.31 | 5.54 | 4.69 | 5.8 | 92 | L5 |
| 17419 | 11.33 | 5.38 | 4.81 | 9.3 | 43 | L5 |
| 17442 | 11.62 | 5.43 | 5.35 | 10.6 | 34 | L5 |
| 17492 | 10.10 | 5.42 | 5.07 | 10.3 | 70 | L5 |
| 18037 | 11.50 | 5.51 | 5.21 | 10.3 | 37 | L5 |
| 18054 | 10.85 | 5.19 | 4.74 | 10.3 | 50 | L5 |
| 23463 | 11.57 | 5.27 | 5.05 | 10.9 | 34 | L5 |
| 23549 | 11.54 | 5.10 | 4.76 | 11.0 | 35 | L5 |
| 24018 | 11.65 | 5.44 | 4.95 | 9.7 | 36 | L5 |
| 24022 | 12.12 | 5.66 | 5.12 | 9.0 | 30 | L5 |
| 24449 | 11.96 | 5.36 | 4.94 | 10.2 | 30 | L5 |
| 24451 | 10.33 | 5.89 | 5.39 | 8.8 | 70 | L5 |
| 24452 | 11.78 | 5.01 | 4.63 | 11.1 | 31 | L5 |
| 24456 | 11.86 | 5.33 | 4.90 | 10.2 | 31 | L5 |
| 24531 | 11.79 | 5.76 | 5.57 | 9.9 | 33 | L4 |
| 25344 | 11.54 | 5.62 | 5.11 | 9.2 | 39 | L5 |
| 25347 | 11.44 | 5.57 | 5.32 | 10.2 | 38 | L5 |
| 29314 | 11.84 | 5.46 | 5.02 | 9.9 | 32 | L5 |
| 30498 | 11.78 | 5.70 | 5.33 | 9.7 | 34 | L5 |
| 30499 | 12.16 | 5.32 | 5.06 | 10.7 | 26 | L5 |
| 30505 | 11.60 | 5.32 | 4.76 | 9.5 | 37 | L5 |
| 30506 | 11.06 | 5.43 | 5.24 | 10.6 | 44 | L5 |
| 30704 | 11.20 | 5.34 | 4.85 | 9.8 | 43 | L5 |
| 30942 | 11.20 | 5.17 | 4.64 | 10.0 | 43 | L5 |
| 31806 | 11.73 | 5.67 | 5.29 | 9.7 | 34 | L5 |
| 31814 | 12.16 | 5.65 | 5.10 | 8.9 | 30 | L5 |
| 31819 | 11.65 | 5.14 | 4.57 | 9.8 | 36 | L5 |
| 31820 | 12.46 | 5.50 | 5.03 | 9.6 | 25 | L5 |
| 32482 | 11.36 | 5.26 | 4.66 | 9.2 | 42 | L5 |
| 32496 | 10.30 | 5.63 | 5.17 | 9.5 | 68 | L5 |
| 32811 | 11.14 | 5.00 | 4.64 | 11.2 | 41 | L5 |
| 47962 | 12.04 | 5.54 | 4.95 | 8.9 | 32 | L5 |
| 51364 | 11.42 | 4.95 | 4.34 | 9.9 | 39 | L5 |
| 53436 | 11.36 | 5.21 | 4.35 | 6.4 | 54 | L4 |
| 55060 | 11.41 | 5.34 | 4.83 | 9.6 | 40 | L5 |
| 55419 | 11.12 | 5.51 | 4.98 | 9.1 | 47 | L5 |
| 65216 | 12.49 | 5.44 | 4.54 | 5.2 | 36 | L4 |
| 67065 | 12.02 | 5.20 | 4.30 | 5.3 | 44 | L4 |
| 69437 | 11.89 | 5.55 | 5.10 | 9.7 | 32 | L5 |
| 73677 | 11.99 | 5.27 | 4.70 | 9.6 | 31 | L5 |
| 85798 | 11.89 | 5.45 | 4.57 | 5.6 | 45 | L4 |
| 1999 XJ55 | 12.21 | 5.29 | 4.42 | 6.0 | 38 | L4 |
| 2000 TG61 | 12.23 | 5.47 | 4.92 | 9.2 | 28 | L5 |
| 2000 SJ350 | 12.55 | 5.44 | 5.03 | 10.0 | 23 | L5 |
| 2001 QZ113 | 11.98 | 5.39 | 4.98 | 10.2 | 30 | L5 |
| 2001 XW71 | 12.71 | 5.51 | 4.89 | 8.7 | 23 | L5 |
| 2001 QQ199 | 12.59 | 6.36 | 5.48 | 4.6 | 37 | L5 |
| 2004 BV84 | 12.95 | 5.37 | 4.74 | 8.8 | 21 | L5 |
| 2004 FX147 | 12.61 | 5.25 | 4.39 | 6.0 | 31 | L4 |
| 2005 EJ133 | 12.72 | 5.39 | 4.80 | 9.1 | 23 | L5 |

Note.—Table 3 is also available in machine-readable form in the electronic edition of the *Astronomical Journal*.

[a] Absolute magnitude (see eq. [1]).

[b] Heliocentric distance.

[c] Geocentric distance.

[d] Phase angle.

[e] Effective diameter (see eq. [2]).

$0.98 \pm 0.02$ mag centered at a mean of $10.64 \pm 0.01$ mag, while asteroid (29314) had a peak-to-peak light-curve amplitude of $1.05 \pm 0.03$ centered on $11.89 \pm 0.02$ mag.

To complete the light-curve study, we continued optical observations of both candidate contact binary asteroids in 2006. Figures 10–13 show the results of the photometric observations.

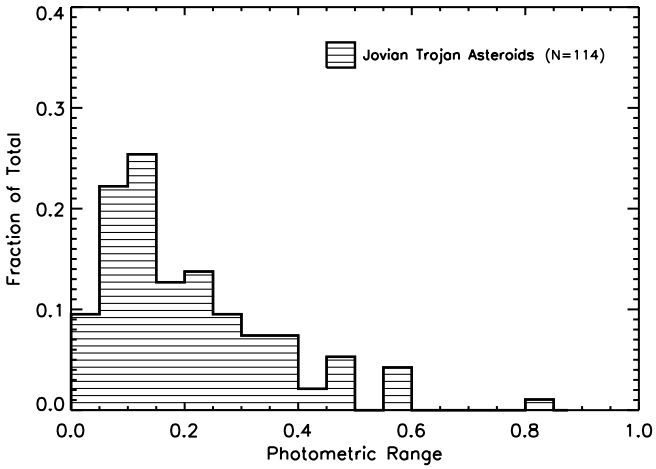


FIG. 4.—Histogram of the distribution of photometric ranges found from sparse-sampled observations of 114 Jovian Trojan asteroids.

In 2006, asteroid (17365) showed a photometric range of 0.81 ± 0.02 mag centered at a mean absolute magnitude of 10.76 ± 0.01. Asteroid (29314) showed a peak-to-peak amplitude of 0.86 ± 0.03 mag with a mean absolute magnitude of 11.80 ± 0.02.

The phase dispersion minimization (PDM) method (Stellingwerf 1978) was used to determine possible rotation periods for each asteroid. Figures 14 and 15 show plots of Θ, which characterizes the dispersion in the data phased to a given period (see Stellingwerf 1978 for more information). The most likely rotation periods corresponded to the smallest values of Θ. Several periods appeared to minimize Θ, but when used to phase the data, the results were not persuasive light curves. In fact, only two periods per asteroid produced convincing light-curve results. For Trojan (29314), minima consistent with the data occur at periods of 0.3133 ± 0.0003 days (7.518 ± 0.007 hr) and a double-peaked period of 0.6265 ± 0.0003 days (15.035 ± 0.007 hr). Asteroid (17365) shows a single-peaked light-curve period of 0.2640 ± 0.0004 days (6.336 ± 0.009 hr) and a double-peaked period of 0.52799 ± 0.0008 days (12.672 ± 0.019 hr).

While both the single-peaked and double-peaked periods produce good fits for Trojan asteroid (29314), the double-peaked light curve is more convincing. The light curve of (29314) shows subtle differences in the shapes of the two minima, which

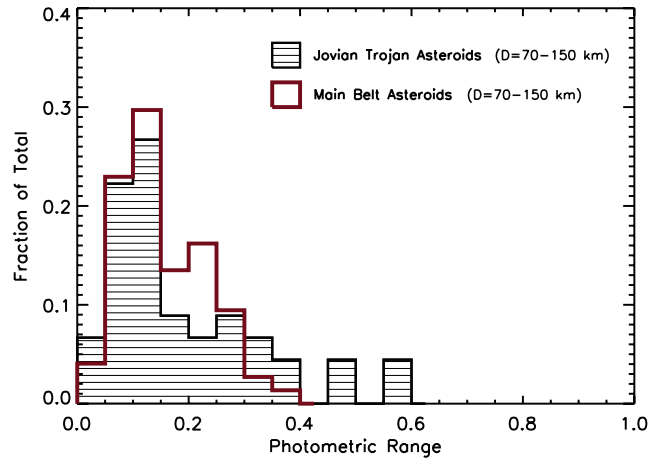


FIG. 5.—Histogram of the photometric ranges of Jovian Trojan asteroids and main-belt asteroids with diameters between 70 and 150 km. Data for main-belt asteroids are taken from Barucci et al. (2002).

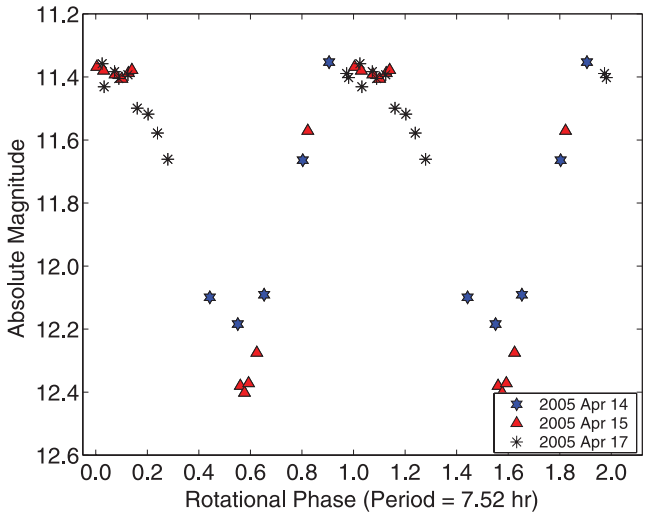


FIG. 6.—Absolute magnitude (calculated from eq. [1]) of Trojan asteroid (29314) in 2005 April. Data are phased to a single-peaked light-curve period of 7.52 hr.

are obvious by the spread in the data when phased to the single-peaked period (see Figs. 10 and 11). Asteroid (17365) shows a more obvious double-peaked light curve (see Figs. 12 and 13) with maxima of different shapes. The maxima of (17365) differ by 0.10 ± 0.01 mag, while the minima differ by 0.06 ± 0.01 mag.

### 3.1. *Candidate Contact Binary Asteroids*

Trojan asteroids (17365) and (29314) show strong evidence of being contact binaries. Both asteroids reveal photometric ranges greater than 0.9 mag, sufficiently long rotation periods (<2 rotations day$^{-1}$), and light-curve profiles (qualitatively similar to 624 Hektor) containing U-shaped maxima and V-shaped minima. Here we speculate about all possible explanations for the brightness variations in the light-curve observations of these Trojan asteroids, including albedo variations, elongated shapes, and binarity (Dunlap & Gehrels 1969; Cook 1971; Hartmann & Cruikshank 1978; Weidenschilling 1980).

Surface albedo contrasts provide a possible but unconvincing explanation for the large brightness variations of the Trojans. Among solar system objects, only Iapetus, a satellite of Saturn,

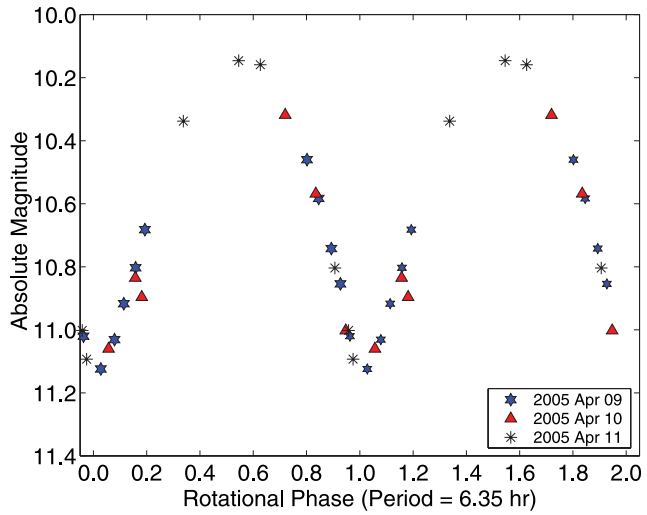


FIG. 7.—Absolute magnitude (see eq. [1]) of Trojan asteroid (17365) in 2005 April. Data are phased to a single-peaked light-curve period of 6.35 hr.

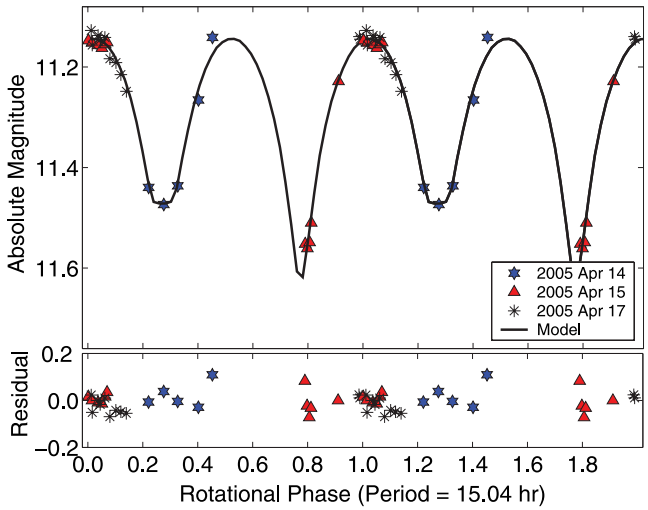


FIG. 8.—Absolute magnitude (see eq. [1]) of Trojan asteroid (29314) in 2005 April. Data are phased to a double-peaked light-curve period of 15.04 hr. The best-fit Roche binary equilibrium model is overplotted.

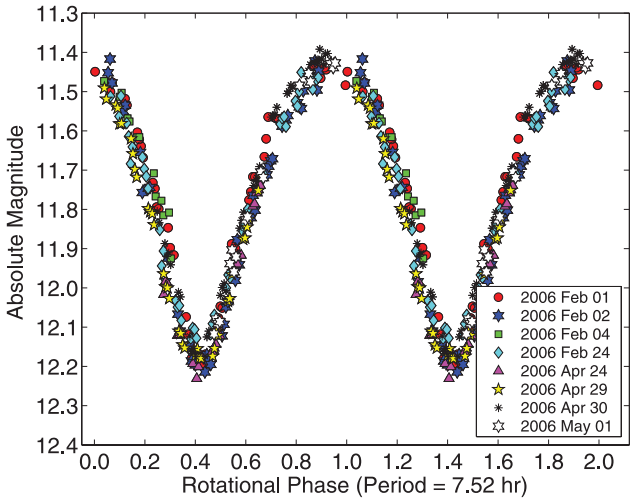


FIG. 10.—Absolute magnitude (see eq. [1]) of Trojan asteroid (29314) between 2006 February and May. Data are phased to a single-peaked light-curve period of 7.52 hr.

shows strong spatial albedo variations which account for its large light-curve amplitude. However, Iapetus's synchronous rotation about Saturn plays a large role in producing the dichotomous behavior of the satellite (Cook & Franklin 1970), and this circumstance is not relevant in the context of the Trojan asteroids. Among previously studied asteroids, double-peaked light curves are almost always caused by rotational variations in the projected area and reflect the elongated shapes of the bodies. While albedo contrasts cannot be formally ruled out, we feel that they are an unlikely cause of the observed brightness variations.

Increasing evidence suggests asteroids have little or no internal strength, probably as a result of impacts that disrupt but do not disperse the object (Farinella et al. 1981; Pravec et al. 2002). The Trojan asteroids have undergone a collisional history that is either similar to that of the main-belt asteroids (Marzari et al. 1997) or perhaps even more intense (Davis et al. 2002; Barucci et al. 2002), making it highly probable that they, too, are gravity-dominated "rubble piles," strengthless or nearly so in tension (Farinella et al. 1981). Studies have found that only the smallest main-belt asteroids, with diameters less than 0.15 km, have sufficient internal strength to overcome gravity (Pravec et al. 2002). Figure 5 from Pravec et al. (2002) shows observations of decreasing maximum spin rate with increasing light-curve amplitude (a proxy for elongation) of near-Earth asteroids. This observation indicates a lack of fast-rotating elongated bodies, which implies that asteroids larger than ~0.15 km are structurally weak and lack the tensile strength to withstand high rotation rates without becoming unstable and flying apart. Also evident in Figure 5 of Pravec et al. (2002) is the tendency of fast rotators to have spheroidal shapes, an indicator of gravity-dominated bodies which do not possess the internal strength to resist gravity. Collectively, the observations point to asteroids being bodies of negligible strength, whose shapes are dominated by rotation and gravity.

Rotation rates must lie between four and six rotations per day in order for rotational elongation of a structurally weak body to be maintained. This is the range for which Jacobi ellipsoids are possible figures of equilibrium (Leone et al. 1984; Farinella & Zappalà 1997). If the rotation rate were much higher than six

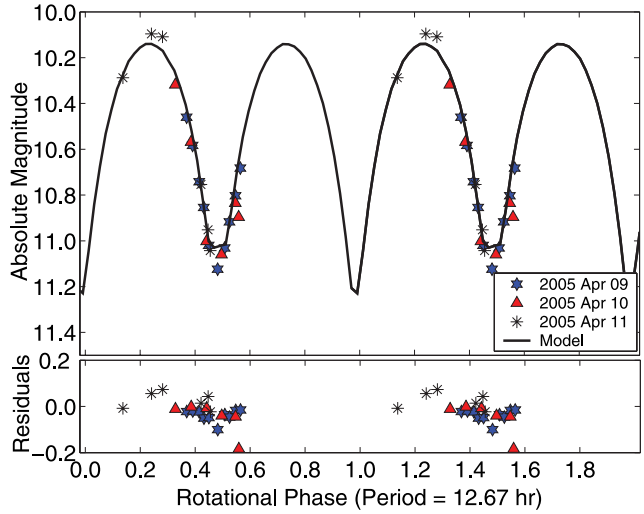


FIG. 9.—Absolute magnitude (see eq. [1]) of Trojan asteroid (17365) in 2005 April. Data are phased to a double-peaked light-curve period of 12.67 hr. The best-fit Roche binary equilibrium model is overplotted.

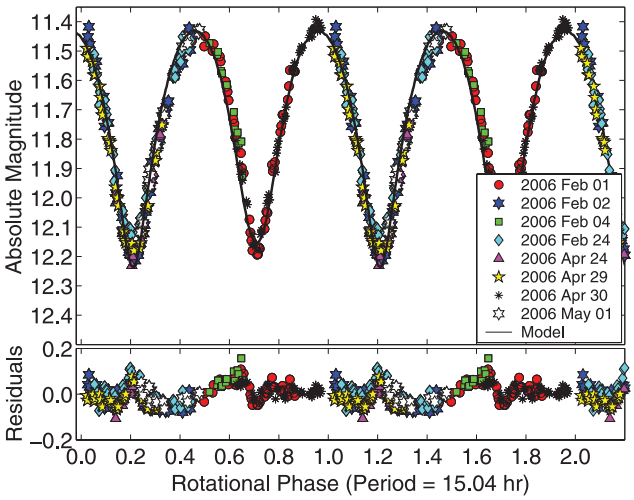


FIG. 11.—Absolute magnitude (see eq. [1]) of Trojan asteroid (29314) between 2006 February and May. Data are phased to a double-peaked light-curve period of 15.04 hr. The best-fit Roche binary equilibrium model is overplotted.

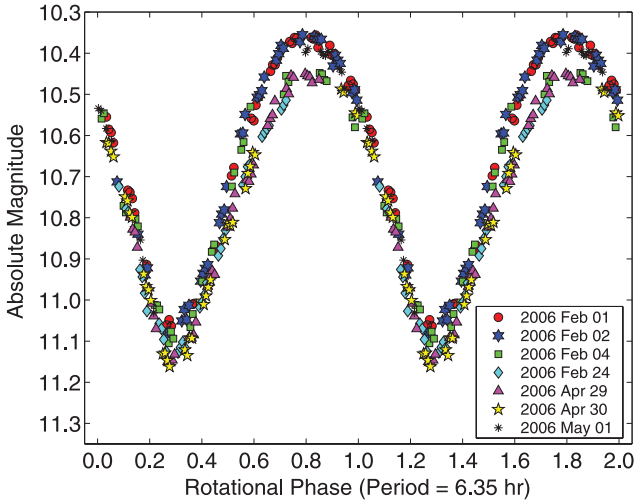


FIG. 12.—Absolute magnitude (see eq. [1]) of Trojan asteroid (17365) between 2006 February and May. Data are phased to a single-peaked light-curve period of 6.35 hr.

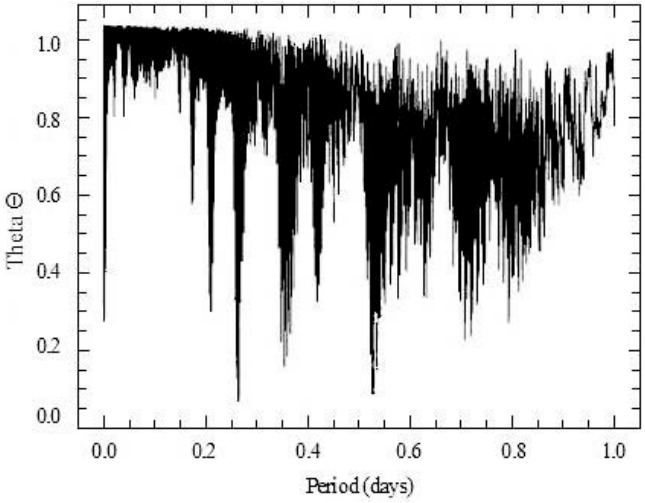


FIG. 14.—PDM plot for Trojan asteroid (17365) showing Θ vs. period. Probable periods are at minimum Θ values: 0.2640 ± 0.0004 and 0.52799 ± 0.0008 days.

rotations per day, the body would fall apart, while at a much lower rotation rate, the body would adopt a spherical figure of equilibrium. In 2005, both asteroids (17365) and (29314) showed photometric variations larger than 0.9 mag, above the threshold for rotational instability in a structurally weak body. In addition, both asteroids have double-peaked light-curve periods that are too slow to cause sufficient rotational elongation. Both observations indicate that rotationally induced elongation is an insufficient explanation for the brightness variations of these Trojan asteroids.

We are therefore left with the strong possibility that Trojan asteroids (29314) and (17365) are contact binaries. Figure 16 is a plot of rotation periods and photometric ranges of several well-studied Kuiper Belt objects and main-belt asteroids. It is divided into three main regions. Region A spans the photometric ranges that can be explained by albedo variations, elongation, or binarity of an asteroid. Region B represents the characteristics explained by albedo variations or rotational elongation of an object, while variations in region C can only be explained by binary asteroids. Both Trojan asteroids lie well within region C, alongside contact binaries 216 Kleopatra, 624 Hektor, and 2001 $QG_{298}$, contributing to their suspected binary nature.

The light curve of a contact binary is expected to show U-shaped or spread-out maxima and V-shaped or notched minima, as shown by the light curves of 2001 $QG_{298}$ (see Sheppard & Jewitt 2004) and 624 Hektor (see Fig. 17). These characteristic light-curve profiles are unlike the distinctive "notched" profile expected for wide, eclipsing binaries, which remain flat for the majority of the orbit and contain sharp dips during the relatively short eclipsing events. The photometric observations of Trojan asteroids (29314) and (17365) are consistent with the light-curve profiles expected of very close or contact binary systems.

The contact binary 624 Hektor was recently discovered to possess a satellite of diameter 15 km using Keck Laser Guide Star Adaptive Optics (Marchis et al. 2006a), but an independent density estimate derived from the orbital motion of this satellite has not yet been published. In addition, the imaging observations of 624 Hektor indicate that its primary component has a double-lobed nature. Similarities are obvious between the light curves of (29314), (17365), and 624 Hektor (see Figs. 11, 13,

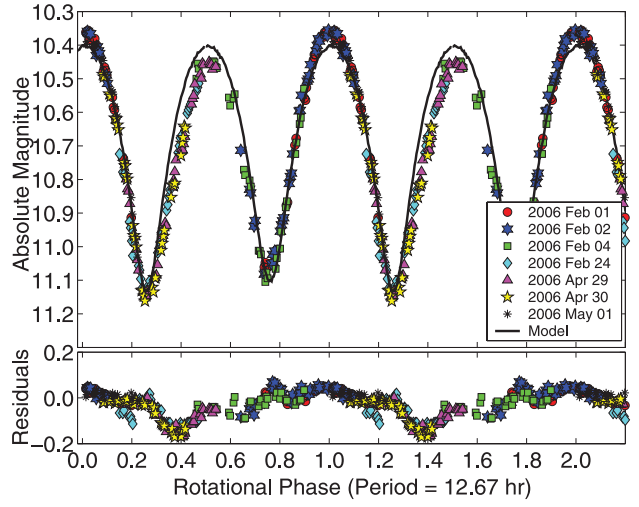


FIG. 13.—Absolute magnitude (see eq. [1]) of Trojan asteroid (17365) between 2006 February and May. Data are phased to a double-peaked light-curve period of 12.67 hr. The best-fit Roche binary equilibrium model is overplotted.

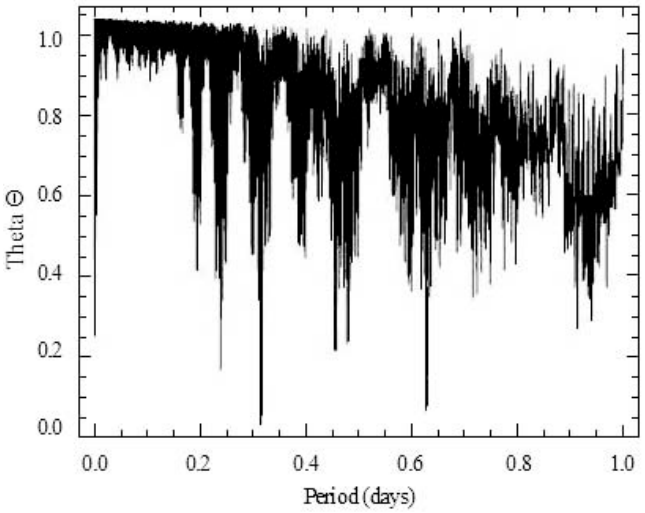


FIG. 15.—PDM plot for Trojan asteroid (29314) showing Θ vs. period. Probable periods minimize Θ: 0.3133 ± 0.0003 and 0.6265 ± 0.0003 days.

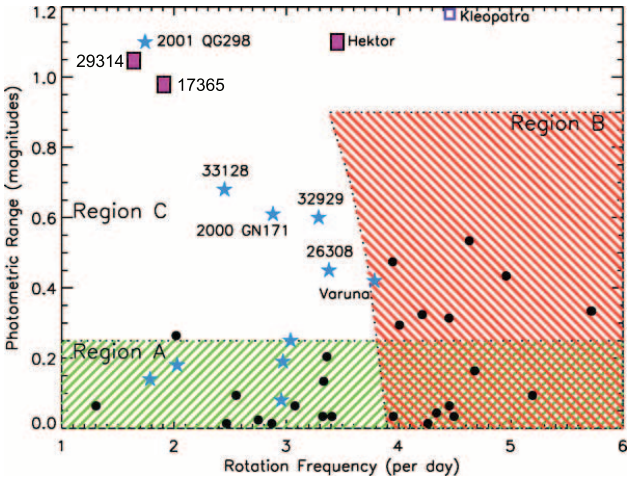


FIG. 16.—Modification of Fig. 5 from Sheppard & Jewitt (2004; originally taken from Leone et al. 1984) to include contact binary candidates (17365) and (29314). Stars represent Kuiper Belt objects, black circles represent main-belt asteroids with diameters larger than 50 km, and pink squares represent the candidate binary Trojans (17365), (29314), and 624 Hektor. Region A includes all objects whose photometric range could be caused by albedo, elongation, or binarity. Region B contains objects that are likely to be rotationally elongated. Only binaries are expected in region C.

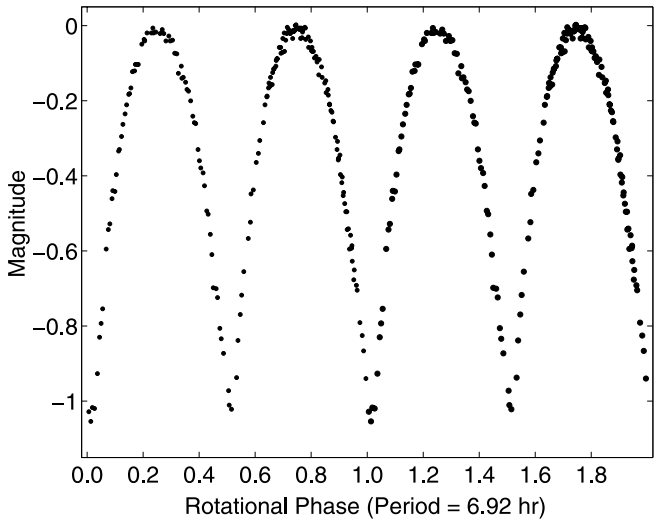


FIG. 17.—Light curve of 624 Hektor in 1968 April, taken from Dunlap & Gehrels (1969). Note the similarities between the light curves of (29314), (17365), and 624 Hektor.

and 17) and consistent with our interpretation that the latter two asteroids are contact binaries.

We used equilibrium models of Roche binaries to determine how well the photometric observations of (17365) and (29314) could be matched by theoretical light curves of contact binary systems. A Roche binary consists of a pair of homogeneous bodies in hydrostatic equilibrium orbiting each other. A strength of this modeling is the ability to estimate densities for the asteroids without knowing the sizes of the binary components. The exact shapes and rotation rates of the Roche binaries were calculated using the mathematical description presented in Leone et al. (1984; see also Chandrasekhar 1987). Binary configurations were calculated for secondary-to-primary mass ratios from $q = 0.25$ to $q = 1.00$ in steps of 0.01. For each value $q$, equations (1)–(3) of Leone et al. (1984) were solved simultaneously to find possible shapes and orbital frequencies for the primary. The same equations were then solved using mass ratio $q' = 1/q$ to calculate the shapes and orbital rates for the secondary. Finally, valid binaries are uniquely selected by matching pairs $(q, 1/q)$ with the same orbital frequency. This procedure is described in detail in Leone et al. (1984) and Lacerda & Jewitt (2007).

The models were ray-traced using the publicly available software POV-Ray,[1] but the surface-scattering routine of POV-Ray was rewritten to allow better control of the scattering function. The scattering law used here was first implemented by Kaasalainen et al. (2001). It linearly combines single (Lommel-Seeliger) and multiple (Lambert) scattering terms using a parameter $k$ (Takahashi & Ip 2004), which varies from 0 to 1. The resulting reflectance function is

$$r \propto (1 - k)\frac{\mu_0}{\mu_0 + \mu} + k\mu_0, \qquad (3)$$

where $\mu_0$ and $\mu$ are the cosines of the incidence and emission angles. When $k = 0$, only single scattering is present, while $k = 1$ simulates pure multiple scattering of light off the surface of the binaries. All binary configurations were ray-traced for $k$ between 0 and 1 in steps of 0.1. Two viewing geometries were modeled, at aspect angles of 75° and 90° (equator-on). The aspect angle lies between the line of sight of the observations and the rotation axis of the body. Simulated illumination angles were chosen to match the phase angles at the time the data were taken. In total, nearly 50,000 models were computed for comparison with the data.

Observations of (17365) and (29314) were simultaneously fitted for the different viewing orientations in 2005 and 2006 to find the best shape interpretation for the asteroids. We assumed that the objects were viewed equatorially in 2005, thus producing the larger photometric range in the discovery epoch data. This assumption was encouraged by the fact that an aspect angle of 75° (rather than 90°) produced a better fit with the 2006 observations (see Figs. 10 and 12).

Figures 8, 9, 11, and 13 show the best-fit models overlaying the light-curve data, with residuals plotted underneath. Best-fit models were found by minimizing $\chi^2$. Small deviations (∼0.1 mag) from the binary model are evident for both asteroids but are negligible compared with the total range of the observations, the more important parameter. Presumably, the deviations are caused by irregularities on the surface of the asteroids, which were not included in the simple binary model but without which the asteroids would be considered odd. The ability of the models to simultaneously fit two epochs of photometric observations lends strong support to the idea that we observed contact binary asteroids over 2 years at different viewing geometries.

Figures 18 and 19 show the shapes derived from the binary models for (29314) and (17365), respectively. Orbital periods combined with shape information allowed us to estimate the densities of the asteroids. The components of our model of asteroid (29314) were found to have a mass ratio of $0.4^{+0.5}_{-0.1}$ and a density of $590^{+40}_{-80}$ kg m$^{-3}$, while our best model of asteroid (17365) has a mass ratio of $0.6^{+0.2}_{-0.1}$ and a density of $780^{+50}_{-80}$ kg m$^{-3}$. These low densities suggest porous asteroid interiors. If (29314) and (17365) have a rock/ice composition similar to the moons of Jupiter, (29314) would have a porosity of ∼64%, while (17365) would have a smaller porosity of 50% (see Fig. 3 from Marchis et al. 2006b). If (17365) and (29314) were composed purely of water ice, their porosities would be 15% and 35%, respectively (Marchis et al. 2006b). This pure water ice composition is unrealistic, however. It is interesting to note that our low-density measurements are consistent with 617 Patroclus (Marchis et al. 2006b).

[1] Available at http://www.povray.org.

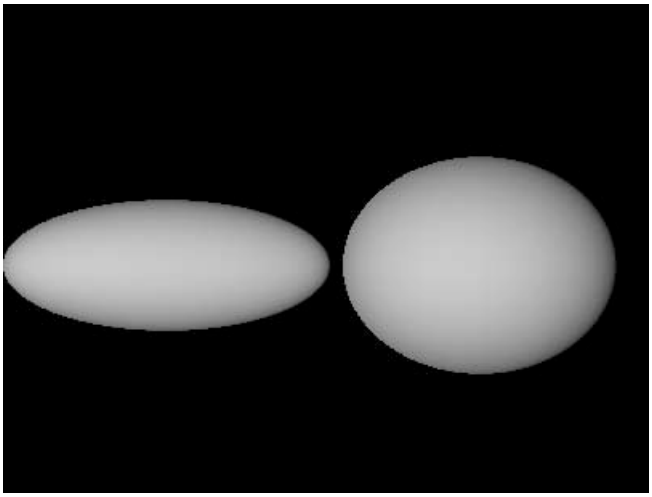

FIG. 18.—Shape interpretation of Trojan asteroid (29314) from Roche binary equilibrium models.

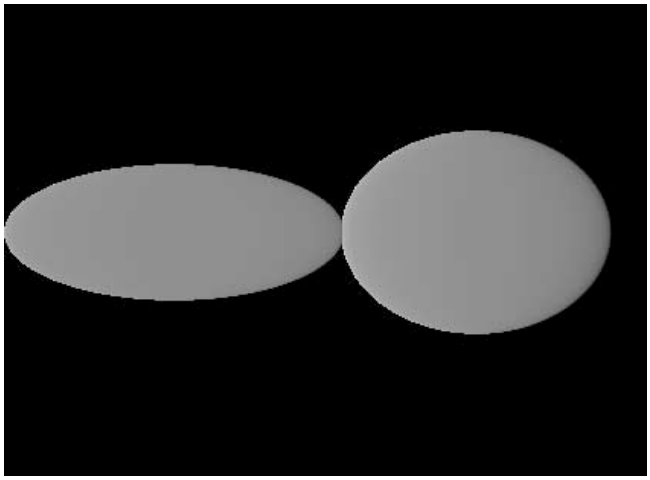

FIG. 19.—Shape interpretation of Trojan asteroid (17365) from Roche binary equilibrium models.

Among the Trojans, only 624 Hektor is known to have a comparable light-curve amplitude, making (29314) and (17265) the second and third known Trojans to show such large rotational variations (see Table 4 for a summary of the candidate binary Trojan asteroid properties). Light-curve analysis suffers from the notorious nonuniqueness problem, which arises from the ability to reproduce any light curve with a complicated pattern of surface markings and shapes. Our interpretation is not unique, but it is the simplest, most plausible explanation for the behavior of the Trojan asteroids.

## 4. DISCUSSION: BINARY FRACTION

Following the method outlined in Sheppard & Jewitt (2004) to account for the geometric circumstances of the observations, we were able to estimate the fraction of contact binary systems among the Jovian Trojan asteroids. This method uses two very crude approximations. In the first approximation, the binary system is simplified to be an elongated, rectangular object with dimensions $a \geq b = c$, with a light-curve amplitude as follows:

$$\Delta m = 2.5 \log\left(\frac{1 + \tan\theta}{b/a + \tan\theta}\right). \quad (4)$$

The range of light-curve amplitudes used to identify contact binary asteroids is 0.9–1.2 mag. For the maximum amplitude of 1.2 mag and viewing angle of $\theta = 0^\circ$, an axis ratio of $a/b = 3$ is calculated from equation (4). Using this axis ratio and the minimum expected amplitude of 0.9 mag, a viewing angle of $10^\circ$ is determined. Therefore, the range of light-curve amplitudes expected for a contact binary asteroid would only be observed if the Earth lay within $10^\circ$ of the equator of the asteroid. The probability that the Earth would lie within $10^\circ$ of the equator of a randomly oriented asteroid is $P(\theta \leq 10^\circ) = 0.17$. We found two suspected contact binary asteroids in our sample of 114 Trojan asteroids, so the fraction of contact binary Jovian Trojan asteroids is approximately $2/114(0.17) = 10\%$.

A second approximation uses an ellipsoid shape to represent the contact binary asteroid, again with dimensions $a \geq b = c$ and a light-curve amplitude expressed by the following:

$$\Delta m = 2.5 \log\left(\frac{a}{b}\right) - 1.25 \log\left\{\left[\left(\frac{a}{b}\right)^2 - 1\right]\sin^2\theta + 1\right\}. \quad (5)$$

Using the axis ratio of $a/b = 3$, in order to observe photometric ranges between 0.9 and 1.2 mag, the Earth must lie within $17^\circ$ of the equator of the ellipsoidal asteroid. The probability of a randomly oriented object having this geometric orientation relative to the observer is $P(\theta \leq 17^\circ) = 0.29$, implying a contact binary fraction of $2/114(0.29) = 6\%$.

We conclude that the fraction of contact binary Trojan asteroids is ~6%–10%. This is a lower limit to the actual fraction, as some of the objects not found to have large amplitudes in the survey sample might in fact have them, because the sparse-sampling method is not 100% efficient. The existence of likely contact binary 624 Hektor separately suggests that the binary fraction is high.

Binaries with equal-sized components are rare in the main belt (the frequency of large main-belt binaries is ~2%; Richardson & Walsh 2006) and have yet to be observed in the near-Earth asteroid population. However, they are abundant in the observed binary Kuiper Belt population, where the fraction lies between 10% and 20% (Sheppard & Jewitt 2004). The results of this study show that there are three Jovian Trojan asteroids that reside in region C. The observations tend to suggest a closer relationship between the binary populations of the Kuiper Belt and the Trojan clouds. This correlation could signify similar binary formation mechanisms in the two populations. This is an interesting connection considering that in one model of formation, the Trojans are actually captured Kuiper Belt objects (Morbidelli et al. 2005). However, it is clear that the total binary fractions in the Kuiper Belt and in the Trojans need to be more tightly constrained before conclusions can be made.

TABLE 4
LIKELY CONTACT BINARY TROJANS

| Asteroid | $\bar{m}(1,1,0)$[a] | $D_e$[b] (km) | $P$ (hr) | $\Delta m$[c] | $\rho$ (kg m$^{-3}$) |
|---|---|---|---|---|---|
| (17365)..... | 10.76 | 92 | 12.672 | 0.98 | 780 |
| (29314)..... | 11.80 | 32 | 15.035 | 1.05 | 590 |
| 624 Hektor..... | 7.37 | 350 × 210 | 6.921 | 1.10 | 2200 |

[a] Mean absolute magnitude (see eq. [1]).
[b] Effective diameter (see eq. [2]).
[c] Maximum photometric range.

The contact binaries detected were skewed toward those with components of comparable sizes, which are capable of producing photometric ranges $\geq$0.9 mag. For mass ratios $\ll$1, sparse sampling would more likely miss the eclipsing event, and the photometric range would be $\leq$0.9 mag and would not attract our attention. The method was strongly dependent on geometric circumstances, and only binaries viewed edge-on or almost equatorially would be detected in our survey. In addition, sparse sampling is only able to put lower limits on the photometric range of an asteroid, making the binary fraction a lower limit estimate. Only binaries with sufficiently short orbital periods (optimally between 6 and 12 hr rotation periods) would be detected, so wide binaries were not accounted for in this study. Therefore, the measured binary fraction is again a strong lower limit to the actual fraction and is suggestive of a significant binary population among the Trojan clouds.

Our project is a pilot study for the much larger scale Pan-STARRS, which will detect every object with a red magnitude brighter than 24 mag. It is estimated that approximately $10^5$ Jovian Trojans exist with red magnitudes lower than 24, all of which will be detected using Pan-STARRS (Jewitt 2003; Ďurech et al. 2005). Our results suggest that Pan-STARRS will reveal between 6000 and 10,000 contact binary systems among the Trojan clouds.

## 5. SUMMARY

Sparsely sampled light-curve measurements were used to statistically study the photometric variations of 114 Jovian Trojan asteroids. Objects with large photometric ranges were targeted for follow-up in this survey and are considered as candidate contact binary systems. Our conclusions are as follows:

1. The sparse-sampling technique successfully confirmed known photometric ranges of both 944 Hidalgo ($0.58 \pm 0.02$ mag) and 2674 Pandarus ($0.50 \pm 0.01$ mag).
2. Two of the 114 observed Trojans, asteroids (17365) and (29314), were found to show photometric ranges larger than expected for rotationally deformed equilibrium figures and were targeted for dense follow-up light-curve observations. The resulting ranges ($0.98 \pm 0.02$ and $1.05 \pm 0.03$ mag, respectively) and long rotation periods ($12.672 \pm 0.019$ and $15.035 \pm 0.007$ hr) of these two Trojans are consistent with a contact binary structure for each object.
3. Roche binary models give densities of $780^{+50}_{-80}$ kg m$^{-3}$ for asteroid (17365) and $590^{+40}_{-80}$ kg m$^{-3}$ for asteroid (29314), suggestive of porous interiors.
4. If (17365) and (29314) are indeed contact binaries, then we estimate from our survey that the binary fraction of the Jovian Trojans is $\sim$6%–10% or more. The total binary fraction (including both wide and close pairs) must be higher.

We thank John Dvorak, Daniel Birchall, Dave Brennan, and Ian Renaud-Kim for operating the UH telescope and Henry Hsieh for assisting with the observations in both Taiwan and Honolulu. We are grateful for the assistance and expertise of the Lulin Observatory staff, in particular Wen-Ping Chen, Chung-Ming Ko, and H. C. Lin. Support for this work by a grant to D. J. from NASA's Origins Program is greatly appreciated.

## REFERENCES

Astakhov, S. A., Lee, E. A., & Farrelly, D. 2005, MNRAS, 360, 401
Barucci, M. A., Cruikshank, D. P., Mottola, S., & Lazzarin, M. 2002, in Asteroids III, ed. W. F. Bottke, Jr., et al. (Tucson: Univ. Arizona Press), 273
Belton, M., et al. 1995, Nature, 374, 785
Binzel, R. P., & Sauter, L. M. 1992, Icarus, 95, 222
Bowell, E., Hapke, B., Domingue, D., Lumme, K., Peltoniemi, J., & Harris, A. W. 1989, in Asteroids II, ed. R. P. Binzel, T. Gehrels, & M. S. Matthews (Tucson: Univ. Arizona Press), 524
Chandrasekhar, S. 1987, Ellipsoidal Figures of Equilibrium (New York: Dover)
Chapman, C. R., et al. 1995, Nature, 374, 783
Cook, A. F. 1971, in IAU Colloq. 12, Physical Studies of Minor Planets, ed. T. Gehrels (Washington: GPO), 155
Cook, A. F., & Franklin, F. A. 1970, Icarus, 13, 282
Cox, A. N. 2000, Allen's Astrophysical Quantities (New York: Springer)
Davis, D. R., Durda, D. D., Marzari, F., Campo, B. A., & Gil-Hutton, R. 2002, in Asteroids III, ed. W. F. Bottke, Jr., et al. (Tucson: Univ. Arizona Press), 545
Dunlap, J. L., & Gehrels, T. 1969, AJ, 74, 796
Ďurech, J., Grav, T., Jedicke, R., Denneau, L., & Kaasalainen, M. 2005, Earth Moon Planets, 97, 179
Farinella, P., Paolicchi, P., Tedesco, E. F., & Zappalá, V. 1981, Icarus, 46, 114
Farinella, P., & Zappalà, V. 1997, Adv. Space Res., 19, 181
Fernández, Y. R., Sheppard, S. S., & Jewitt, D. C. 2003, AJ, 126, 1563
Funato, Y., Makino, J., Hut, P., Kokubo, E., & Kinoshita, D. 2004, Nature, 427, 518
Goldreich, P., Lithwick, Y., & Sari, R. 2002, Nature, 420, 643
Harris, A. W., Lagerkvist, C. I., Zappalá, V., & Warner, B. D. 2006, Minor Planet Lightcurve Parameters (Greenbelt: National Space Science Data Center), http://cfa-www.harvard.edu/iau/lists/LightcurveDat.html
Hartmann, W. K., Binzel, R. P., Tholen, D. J., Cruikshank, D. P., & Goguen, J. 1988, Icarus, 73, 487
Hartmann, W. K., & Cruikshank, D. P. 1978, Icarus, 36, 353
Holsapple, K. A. 2004, Icarus, 172, 272
Ivezic, Z., et al. 2001, AJ, 122, 2749
Jewitt, D. C. 2003, Earth Moon Planets, 92, 465
Jewitt, D. C., Trujillo, C. A., & Luu, J. X. 2000, AJ, 120, 1140
Kaasalainen, M., Torppa, J., & Muinonen, K. 2001, Icarus, 153, 37
Lacerda, P., & Jewitt, D. 2007, AJ, 133, 1393
Landolt, A. U. 1992, AJ, 104, 340
Leone, G., Paolicchi, P., Farinella, P., & Zappalá, V. 1984, A&A, 140, 265
Marchis, F., Wong, M. H., Berthier, J., Descamps, P., Hestroffer, D., Vachier, F., Le Mignant, D., & de Pater, I. 2006a, IAU Circ., 8732, 1
Marchis, F., et al. 2006b, Nature, 439, 565
Marzari, F., Farinella, P., Davis, D. R., Scholl, H., & Campo, B. A. 1997, Icarus, 125, 39
Merline, W. J., et al. 2001, IAU Circ., 7741, 2
Morbidelli, A., Levison, H. F., Tsiganis, K., & Gomes, R. 2005, Nature, 435, 462
Pravec, P., Harris, A. W., & Michalowski, T. 2002, in Asteroids III, ed. W. F. Bottke, Jr., et al. (Tucson: Univ. Arizona Press), 113
Richardson, D. C., & Walsh, K. J. 2006, Annu. Rev. Earth Planet. Sci., 34, 47
Russell, H. N. 1916, ApJ, 43, 173
Sheppard, S., & Jewitt, D. C. 2004, AJ, 127, 3023
Stellingwerf, R. F. 1978, ApJ, 224, 953
Takahashi, S., & Ip, W. H. 2004, PASJ, 56, 1099
Weidenschilling, S. J. 1980, Icarus, 44, 807
———. 1989, in Asteroids II, ed. R. P. Binzel, T. Gehrels, & M. S. Matthews (Tucson: Univ. Arizona Press), 643
———. 2002, Icarus, 160, 212
Yoshida, F., & Nakamura, T. 2005, AJ, 130, 2900